PRAMANA — journal of physics
© Indian Academy of Sciences
Vol. 55, No. 4
October 2000
pp. 545–558

Searching for gravitational waves from rotating neutron stars

S V DHURANDHAR
Inter-University Centre for Astronomy and Astrophysics, Ganeshkhind, Post Bag 4, Pune 411 007, India

Abstract. Rotating neutron stars are one of the important sources of gravitational waves (GW) for the ground based as well as space based detectors. Since the waves are emitted continuously, the source is termed as a continuous gravitational wave (CGW) source. The expected weakness of the signal requires long integration times ($\sim$ year). The data analysis problem involves tracking the phase coherently over such large integration times, which makes it the most computationally intensive problem among all GW sources envisaged. In this article, the general problem of data analysis is discussed, and more so, in the context of searching for CGW sources orbiting another companion object. The problem is important because there are several pulsars, which could be deemed to be CGW sources orbiting another companion star. Differential geometric techniques for data analysis are described and used to obtain computational costs. These results are applied to known systems to assess whether such systems are detectable with current (or near future) computing resources.

Keywords. Gravitational waves; data analysis; neutron stars.

PACS No. 04.30.-w

1. Introduction

The general theory of relativity predicts the existence of gravitational waves. Since gravity couples very weakly to matter, highly sensitive detectors are required to detect gravitational waves. Over the next decade several large-scale interferometric gravitational wave detectors will come online. These include the LIGO, composed of two interferometric detectors situated in the United States each with baselines of 4 km, VIRGO, an Italian/French project located near Pisa with a baseline of 3 km, GEO600, a British/German interferometer under construction near Hannover with a baseline of 600 m, TAMA in Japan, a medium-scale laser interferometer with a baseline of 300 m and with funding approval AIGO500, the proposed 500 m project sponsored by ACIGA [1–5]. There are also separate proposals for space-based detectors which could be operational twenty-five years from now (e.g. LISA: the Laser Interferometer Space Antenna, a cornerstone project of the European Space Agency) [6].

Several types of GW sources have been envisaged which could be directly observed by Earth-based detectors (see [7–9] and references therein for recent reviews): (i) burst sources – such as binary systems of neutron stars (NS) and/or black holes (BH) in their in-spiral phase, BH/BH mergers and supernovae explosions – whose signals last for a time much shorter, typically between a few milli-seconds and a few minutes, (ii) stochastic backgrounds of radiation, either of primordial or astrophysical origin, and (iii) continuous gravitational wave (CGW) sources – emitted by rapidly rotating NS – where a weak deterministic signal is continuously present in the data stream.

In this article data analysis issues concerning CGW sources will be discussed. The data analysis will be applied for investigating the computational load involved in filtering the data stream to search for monochromatic radiation emitted by a NS orbiting a companion object.

CGW emitters pose one of the most computationally intensive problems in GW data analysis. In fact, the weakness of the expected signal requires very long observation times, of the order of a year (or possibly more) in order to accumulate enough signal-to-noise ratio (SNR) for ensuring detection. During this time a monochromatic signal, as measured in the source reference frame, is Doppler modulated by the motion of the detector carried by the spinning Earth orbiting the Sun. The emitted energy is spread over $\simeq 2 \times 10^6 \, (T/10^7 \, \mathrm{sec})^2 \, (f/1 \, \mathrm{kHz})$ frequency bins of width $\Delta f = 1/T$, where T is the time of observation (the formula holds for T up to six months, after that the bins increase linearly with T). In order to recover the whole power in one frequency bin one has to 'correct' the recorded data stream for each possible source position in the sky. The problem is much worse, if the the intrinsic frequency of the source changes, say due to spindown. Then the power is spread over $3 \times 10^6 \, (\tau/10^3 \, \mathrm{yrs})^{-1} \, (T/10^7 \, \mathrm{sec})^2 \, (f/1 \, \mathrm{kHz})$ bins, where $\tau = f/\dot{f}$ is the spin-down age of the NS. Indeed, one then needs to correct also for this effect, searching through one or more of the spin-down parameters. It is clear that searches for CGW are limited by the available computational resources [10,11].

Due to the large computational burden, algorithms investigated so far have been restricted to *isolated* NS ie. NS which are at rest or in uniform motion with respect to the barycentre, but whose GW frequency and location in the sky are unknown. This is called the 'all sky all frequency' search [10]. Even here the computational costs are formidable, typically involving 10^{24} operations, for an intrinsically monochromatic source, where the search carried is up to a maximum GW frequency of 1 kHz and observation time of 10^7 sec. The problem of searching for a CGW emitter orbiting a companion object is simply considered computationally intractable, since up to five more search parameters would be required and this would compound the already enormous computational cost. In this article, we address the complementary problem: we assume that the direction to the source is known, but that the source orbits a companion object. Such a situation manifests itself astrophysically in globular clusters in our galaxy. There are about 200 such clusters whose directions are known. The large ones contain more than a million stars each, a large fraction of them believed to be in binaries. Restricting ourselves to this problem does not sacrifice generality. The general problem in which one must perform a search over directions as well, the number of filters (independent Doppler corrections) is essentially (ignoring correlations between parameters) the product of the number of filters obtained here and the number of directions in the sky over which one must search.

2. Emission of GW from rotating NS

The NS must be non-axisymmetric in order that it radiates gravitationally. Several mechanisms have been envisaged which can give rise to non-axisymmetry in NS. These have been detailed in Brady *et al* [11]. Here we briefly mention the mechanisms. The measure of non-axisymmetry is denoted by ϵ and the characterstic amplitude h of the CGW source is given by

$$h \sim 10^{-25} \left(\frac{I}{10^{45}\mathrm{gm.cm}^2}\right) \left(\frac{f}{1\,\mathrm{kHz}}\right)^2 \left(\frac{\epsilon}{10^{-5}}\right) \left(\frac{r}{10\,\mathrm{kpc}}\right)^{-1}, \tag{1}$$

where I is the moment of inertia of the NS, f the GW frequency and r the distance to the source.

The following mechanisms are envisaged:

1. *Large magnetic fields:* Large magnetic fields not aligned along the spin-axis can produce asymmetry due to the magnetic pressure. $\epsilon \sim 10^{-9}$ is possible by this type of mechanism.

2. *The Chandrasekhar–Friedman–Schutz (CFS) instability and r-modes:* The CFS instability can occur for fast spinning NS, where the instability is driven by gravitational radiation reaction. A similar mechanism which has been recently realised, involves the Rossby (r) - modes. These modes are again driven by the gravitational radiation reaction which couples to the current multipole moments. The h for these modes can be as much as few times $10^{-25}(20\ \mathrm{Mpc}/r)$ [12].

3. *Accretion on to NS:* A far more interesting scenario is the accretion of hot material onto the NS surface. Here the induced quadrupole moment is directly related to the accretion rate, which can be copious. The gravitational energy reservoir, moreover, can be continuously replenished, if continuous accretion occurs. The key idea behind this scenario is that gravitational wave radiation can balance the torque due to accretion, and was proposed over 20 years ago [13,14]. However, it has attracted considerable new interest in the past two years and has been fully revitalized by the launch of the Rossi X-ray timing explorer, designed for precision timing of accreting NS. The observational evidence that low mass X-ray binaries (LMXBs) – binary systems where a NS accretes material from a low mass companion – in our galaxy are clustered around a rotation frequency ≈ 300 Hz, led Bildsten [15] to propose a mechanism to explain this behaviour. The fundamental idea is that continuous emission of GW radiates away the angular momentum that is transferred to the NS by the infalling material. The fact that the rate of angular momentum loss through GW's scales as f^5, provides a very natural justification of the clustering of rotation frequency of several sources. The physical process responsible for producing a net quadrupole moment is the change of composition in the NS crust, which in turn is produced by the temperature gradient caused by the infalling hot material. Recently, Ushomirsky *et al* [16] have posed this initial idea on more solid theoretical grounds. If such mechanism does operate, LMXBs are extremely interesting candidate sources for Earth-based detectors. Several systems would be detectable by LIGO operating in the 'enhanced' configuration (LIGO II), if the detector sensitivity is tuned, through narrow-banding, around the emission frequency. In particular, Sco X-1, the most luminous X-ray source in the sky, possibly is marginally detectable by 'initial' LIGO and GEO600 (the latter in narrow-band configuration), where an integration time of approximately 2 years would be required. The characteristic amplitude for this source is

$$h_{\rm eff} \simeq 4 \times 10^{-27} \left(\frac{R_{\rm NS}}{10^6\,{\rm cm}}\right)^{3/4} \left(\frac{m_{\rm NS}}{1.4\,M_\odot}\right)^{-1/4} \times \left(\frac{F_X}{10^{-8}\,{\rm erg\,cm^{-2}\,sec^{-1}}}\right)^{-1/2}, \tag{2}$$

where $R_{\rm NS}$ is the typical radius of a neutron star and F_X is the X-ray flux.

3. The signal

For a typical CGW source the signal at the detector is essentially sinusoidal. The frequency can change slightly (i) intrinsically by spindown, and/or (ii) Doppler modulation because of the relative motion between the source and the detector. Consider for simplicity a source that is monochromatic in its own rest frame where the changes in intrinsic frequency of the source have been ignored. This problem is sufficiently numerically intensive that any insight gained will be a significant step. Since the observation lasts for a long time $\sim$ a year, the Earth partakes of several motions – rotational, orbital motion about the sun, motion about the moon etc. – the detector being carried with it. Moreover, during the observation time, the source too can change position while orbiting a companion. If the centre of mass (CM) of the binary system is at rest or moves with constant velocity with respect to the barycentre, the phase Φ of the signal has the form

$$\Phi(t) = 2\pi f_0 t + \phi_{\rm D}(t), \tag{3}$$

where

$$\phi_{\rm D}(t) = 2\pi f_0 \left[(\Delta\bar{r}_d(t) + \Delta\bar{r}_s(t))\,.\frac{\hat{\mathbf{n}}(\theta,\phi)}{c}\right]. \tag{4}$$

$\phi_{\rm D}(t)$ is the Doppler phase correction which comprises of two terms $\Delta\bar{r}_d(t)$ and $\Delta\bar{r}_s(t)$ representing the displacements of the detector and source at time t respectively. $\hat{\mathbf{n}}(\theta,\phi)$ is the unit vector pointing from the barycentre to the CM of the binary, f_0 is the constant frequency of the source in the barycentric frame, if the source is held at rest in the CM frame of the binary and $c \simeq 2.9979 \times 10^{10}$ cm/sec is the speed of light. From (3) we observe that, the total phase is the sum of the intrinsic phase $2\pi f_0 t$ and the Doppler phase contribution $\phi_{\rm D}(t)$. Both $\Delta\bar{r}_d(t)$ and $\Delta\bar{r}_s(t)$, in general, can involve complex accelerated motions making the problem of data analysis highly nontrivial. It therefore becomes prudent to divide the problem into relatively simpler special cases, and treat each such case individually.

The signal gravitational strain amplitude $h(t)$ is given by

$$h(t) = \Re[\mathcal{A}\exp(-i\Phi(t) + i\Psi)], \tag{5}$$

where $\Phi(t)$ is given by eq. (3). The polarization amplitude $\mathcal{A}$, and the polarization phase Ψ are slowly varying time-dependent functions over the time-scale of the day and depend on the relative orientations of the source and the detector. In agreement with all the investigations carried out so far, we assume them constant in our analysis. It is expected that these factors can be easily included in the full analysis and will not significantly affect the computational burden [11].

If we set $\Delta\bar{r}_s(t) = 0$, we obtain the case of the *isolated* NS, which has been dealt with extensively in the literature [10,11,17]. The signal is monochromatic in the barycentric frame, but in the detector frame the signal gets phase modulated as the detector is carried along with the Earth which moves with respect to the barycentre. Since $\Delta\bar{r}_d(t)$ is known, the phase modulation profile depends only on the direction $\hat{n}$ to the source, as also the Doppler correction that one must apply. If we can tolerate a SNR loss of say 30%, the correction 'works' for a tiny patch in the sky. This criterion leads to a search of about 10^{13} directions [10] for detecting a kHz GW in a observation time of 10^7 sec. The detector in the meanwhile has traversed the orbit of the Earth. This number is basically the square of the size of the Earth's orbit divided by the minimum wavelength of the gravitational wave that one is interested in detecting. The number of floating point operations that one must perform, even after employing the FFT algorithm, gives the colossal figure of about 10^{24}! As mentioned before the data analysis is then limited by the computing power available. Hierarchical methods are being explored [17,18] in which coherent and incoherent stages are alternated in order to identify cheaply candidates with a suboptimal algorithm. The candidates are then followed up with a coherent but computationally intensive search.

The second special case arises when the direction to the source is taken to be known. Then the motion of the detector can be subtracted out and one has to deal only with the motion of the source (described by the term $\Delta\bar{r}_s(t)$). The source motion is described by the model of the orbit that we assume. For a circular orbit the Doppler phase depends on 3 parameters, while for a Keplerian elliptical orbit the phase depends on 5 parameters. In this article this case will be described in detail in §5.

The third special case is of a NS whose direction and orbit are known. Radio pulsars fall into this category. 706 pulsars are listed in the Princeton catalogue [19]. But they must satisfy the condition that their GW frequency (taken to be twice the electromagnetic frequency) falls within the bandwidth of the detector. Secondly, from the spindown one can compute the upper bound on the amplitude h, by attributing all the spin down to gravitational radiation. For most pulsars this yields low amplitudes $h \lesssim 10^{-26}, 10^{-27}$. For the pulsar PSR 437-4715 which is the nearest millisecond pulsar detailed analyses have been performed [20,21]. For some of the known pulsars few or all of the parameters are known within given error bars. Then the search must be launched only within these parameter ranges, which brings down the computational cost of the search dramatically.

However, pulsar statistics [22] predicts about 200,000 pulsars in our galaxy. Also it is estimated that there could be $\sim 10^8$ NS in our galaxy. Since less than a percent of the pulsars have been observed so far, it is clear that a GW search for unknown NS is highly recommended.

4. The differential geometric formalism for data analysis

In order to accumulate the signal-to-noise (SNR) efficiently it is desirable to track the phase of the signal as accurately as possible during the entire observation time. This is referred to as coherent integration of the signal, where the SNR grows as $T^{1/2}$. This is in contrast with incoherent methods, where one disregards the phase information, and the SNR does not accumulate as quickly. Coherently integrating the signal implies that one must faithfully follow the phase of the signal sufficiently accurately, that is, well within one cycle, perhaps something like a fraction of a radian. If one exactly know the phase of the signal, then this can be easily achieved. However, the problem becomes enormously demanding, if the phase is known only as a function of parameters, where the parameters are constrained to lie within some given range. Since in general the signal may contain a large number of cycles – a kHz signal lasting for 10^7 seconds has 10^{10} cycles – there exist a large number of ways in which the phases could mismatch for different values of the parameters. More precisely if the correlation integral between two signals with different phase developments reduces below some acceptable value, then we call the two phase developments as different.

The above remarks can be elegantly described in a geometrical framework. In the geometrical picture [23,24], the signal is a vector in the vector space of data trains and the N-parameter family of signals traces out an N-dimensional manifold which is termed as the *signal manifold*. The parameters themselves are coordinates on this manifold, which we denote by the N-dimensional parameter vector $\boldsymbol{\lambda}$. One can introduce a metric γ_{jk} on the signal manifold which is related to the fractional loss in the signal to noise ratio when there is a mismatch of parameters between the signal and the filter. The spacing of the grid of filters is decided by the fractional loss due to the imperfect match that can be tolerated. Given the parameter space that one needs to scan, it is then easy to estimate the total number of filters required to carry out the search for the signal. In §4, we first briefly review the method introduced by Brady *et al* [11] which in turn was based on Owen's [25] method for searching for GW signals from in-spiralling compact binaries. We present here a rigourous approach based on differential geometric methods.

4.1 *Number of filters*

In this approach, the idea is to first correct for the Doppler effect in the phase for each of the grid points of the parameter space and then compute the power spectrum. The power spectrum is obtained efficiently via the FFT algorithm. Even if we know the frequency of the pulsar, it is desirable to search over frequencies over a band of a percent of the pulsar frequency [26]. We therefore have a large number of frequency bins to search over and the FFT algorithm is computationally advantageous. If the Doppler correction is right, that is, if the signal and filter parameters match perfectly, then the signal is all concentrated at $f = f_0$ in the power spectrum. The grid spacing is decided by the amount the maximum of the power spectrum falls when the parameters of the signal and filter mismatch. The mismatch μ is defined as the fractional reduction in the maximum of the power spectrum when the parameters mismatch. Fixing the mismatch μ, fixes the grid spacing of the filters in the parameter space which we will denote by $\mathcal{P}$. The number density of filters (the number of filters per unit proper volume – proper volume defined through the metric) in $\mathcal{P}$ depends on μ, and is denoted by $\rho_N(\mu)$, where N is the dimension of $\mathcal{P}$. For a hyper-rectangular mesh, we have

$$\rho_N(\mu) = \left[2\sqrt{\frac{\mu}{N}}\right]^{-N} . \tag{6}$$

The proper volume of $\mathcal{P}$, can be easily computed from the metric γ_{jk} on $\mathcal{P}$ [11]

$$V_{\mathcal{P}} = \int_P \mathrm{d}\boldsymbol{\lambda}\, \sqrt{\det ||\gamma_{jk}||}\,. \tag{7}$$

The number of filters $\mathcal{N}$ is then just the proper volume eq. (7), times the filter density eq. (6):

$$\mathcal{N} = \rho_N(\mu) V_{\mathcal{P}}\,. \tag{8}$$

For the Keplerian elliptical orbit we have $N = 5$, while for the circular case the dimension of $\mathcal{P}$ reduces to $N = 3$. For a mismatch $\mu = 0.03$, $\rho_3(\mu)$ is 125 and $\rho_5(\mu) \sim 10^4$.

4.2 *The general form of the metric*

If the signal parameters are $(f_0, \boldsymbol{\lambda})$ denoted together by $\boldsymbol{\Lambda}$ and the filter parameters are $\boldsymbol{\lambda} + \Delta\boldsymbol{\lambda}$, the power spectrum $P(f)$ for an observation time T is given by

$$P(f; f_0, \boldsymbol{\lambda}, \Delta\lambda) = \frac{\mathcal{A}^2}{T} \left| \int_0^T \mathrm{d}t\, \exp[i\Phi(t; \boldsymbol{\lambda}, \Delta\boldsymbol{\lambda})] \right|^2\,, \tag{9}$$

where

$$\Phi(t; \boldsymbol{\lambda}, \Delta\boldsymbol{\lambda}) = 2\pi(f - f_0)t + \phi_{\mathrm{D}}(t; f_0, \boldsymbol{\lambda} + \Delta\boldsymbol{\lambda}) - \phi_{\mathrm{D}}(t; f_0, \boldsymbol{\lambda})\,. \tag{10}$$

The mismatch is both in $\boldsymbol{\lambda}$ as well as in f (this can occur because of sampling at the wrong frequency) and is denoted by $m(\boldsymbol{\Lambda}, \Delta\boldsymbol{\Lambda})$

$$\begin{aligned} m(\boldsymbol{\Lambda}, \Delta\boldsymbol{\Lambda}) &\equiv 1 - \frac{P(f; f_0, \boldsymbol{\lambda}, \Delta\boldsymbol{\lambda})}{P(f_0; f_0, \boldsymbol{\lambda}, \bar{0})}\,, \\ &\simeq g_{\alpha\beta}(\boldsymbol{\Lambda})\Delta\Lambda^\alpha \Delta\Lambda^\beta + o(\Delta\boldsymbol{\Lambda}^3)\,. \end{aligned} \tag{11}$$

From eqs (9) and (11) the metric $g_{\alpha\beta}$ can be computed by Taylor expansion. It is given by

$$g_{\alpha\beta} = \langle \Phi_\alpha \Phi_\beta \rangle - \langle \Phi_\alpha \rangle \langle \Phi_\beta \rangle, \tag{12}$$

where the suffix, say α, denotes derivative with respect to $\Delta\Lambda^\alpha$ and the angular brackets denote time averages defined as follows: For a function $X(t)$ defined on the data train $[0, T]$, the time average of X is

$$\langle X \rangle = \frac{1}{T} \int_0^T \mathrm{d}t\, X(t)\,. \tag{13}$$

We remark that $g_{\alpha\beta}$ is not the metric which is used to calculate the proper volume, because it still includes f. We need to maximize over f, which is tantamount to projecting $g_{\alpha\beta}$ orthogonal to the Δf direction. Thus the metric on the submanifold of the search parameters $\boldsymbol{\lambda}$ is

$$\gamma_{ij} = g_{ij} - \frac{g_{0i} g_{0j}}{g_{00}}\,. \tag{14}$$

Here the index 0 identifies the parameter corresponding to the frequency f. If $f_{\max}$ is the highest GW frequency that we are searching for, then we must put $f_0 = f_{\max}$ in the above expression for γ_{ij}. The proper volume of the signal and the total number of templates can be easily derived by inserting eqs (14) and (6), into eqs (7) and (8), respectively.

5. CGW source orbiting a companion

We investigate in this section the problem of a CGW source orbiting a companion star. The discussion here is largely based on the detailed work by Dhurandhar and Vecchio [27]. We apply the data analysis formalism described in the previous section to obtain the computational costs for Keplerian elliptical orbits, treating circular orbits as an important special case. We finally also discuss targetted searches for the X-ray source Sco X-1 and the 44 known radio pulsars in binaries listed in [19].

5.1 *The signal phase*

Here we first compute the Doppler phase modulation due to the motion of the source. To this end, orient the Cartesian coordinate system (ξ, η, ζ) attached to the binary source, so that: (i) $\mathbf{r}_s(t)$ lies in the (ξ, η) plane with the origin at the centre of the ellipse, (ii) the semi-major axis of the ellipse coincides with the ξ-axis, and (iii) the ζ-axis points in the direction of the orbital angular momentum. We specify the direction to the detector by the unit vector (note this $\hat{\mathbf{n}}$ has opposite direction to the one in eq. (4)):

$$\hat{\mathbf{n}} = (\sin\epsilon\cos\psi)\,\hat{\boldsymbol{\xi}} + (\sin\epsilon\sin\psi)\,\hat{\boldsymbol{\eta}} + (\cos\epsilon)\,\hat{\boldsymbol{\zeta}}\,, \tag{15}$$

where ϵ and ψ are the usual polar angles.

The orbit in the (ξ, η) plane is given as follows: Let a be the *semi-major axes* of the elliptical orbit and e the *eccentricity*, then, the orbit is described by the equations

$$\begin{aligned} \xi(t) &= a\cos E(t), \\ \eta(t) &= a\sqrt{1-e^2}\,\sin E(t), \end{aligned} \tag{16}$$

where $E(t)$ is the so-called *eccentric anomaly*; it is related to the *mean angular velocity* ω by the Kepler equation

$$E(t) - e\sin E(t) = \omega t + \alpha, \tag{17}$$

where α is an initial phase, $0 \le \alpha < 2\pi$. When $\omega t + \alpha = 0$ we have $E = 0$ and the mass is closest to the focus $\xi = ae, \eta = 0$. These equations describe the orbit in the (ξ, η)-plane as function of time, that is determined by the four orbital elements a, ω, α, e. However, the orbit in space requires two additional parameters, namely, the angles ϵ and ψ. Thus in all we have six orbital elements which specify the orbit in space.

The Doppler phase correction is obtained from eq. (4). We assume that we have corrected for Earth's motion, so that it is only the second term in eq. (4) that we must consider,

$$\phi_{\mathrm{D}}(t) = -\frac{2\pi f_0 a\sin\epsilon}{c}\left[\cos\psi\cos E(t) + \sin\psi\sqrt{1-e^2}\sin E(t)\right]. \tag{18}$$

The t here can be regarded as the barycentric time. The parameters over which one must launch a search are not exactly the orbital elements, and need not be of the same number. It is the Doppler phase correction that is observed and so the information about the system that we can glean depends on the combination of the orbital elements that enter into it. The

a and ϵ combine into a single parameter $a \sin \epsilon \equiv a_p$, the projected semi-major axis along the line of sight, which is actually the quantity inferred from astrophysical observations. The other search parameters are the remaining orbital elements ω, α, e and ψ. So *in the general case*, when we do not know any of the parameters exactly, we have a *5-dimensional parameter space* to search.

We note that f_0 is not a search parameter because of the special search technique that is employed [11]: it involves 'stretching' the time coordinate in such a way, so as to make the signal appear monochromatic in this time coordinate. One then simply takes the FFT to compute the power spectrum, which now is concentrated in a single frequency bin. It is convenient for the purposes of computation to express the phase $\Phi(t)$, eq. (10), in terms of dimensionless parameters. We write

$$\Phi = (2\pi f_0 T)\, \tilde{\Phi}, \tag{19}$$

where

$$\tilde{\Phi} = \kappa u + X \cos E + Y \sqrt{1 - e^2} \sin E\,, \tag{20}$$

and the dimensionless parameters are given by $u = t/T$, $\kappa = (f - f_0)/f_0$, $X = -a \sin \epsilon \cos \psi / cT$, $Y = -a \sin \epsilon \sin \psi / cT$ and $\Omega = \omega T$. Here u is a dimensionless time satisfying $0 \leq u \leq 1$. So now the new set of parameters is $\boldsymbol{\Lambda} = (\kappa\,, X\,, Y\,, e\,, \Omega\,, \alpha)$ and $\boldsymbol{\lambda} = (X\,, Y\,, e\,, \Omega\,, \alpha)$.

The exact expression for the determinant is quite complicated. There are two relevant regimes: (i) $\Omega \gg 1$ and (ii) $\Omega \ll 1$ in which one obtains simple enough expressions and which are useful over most of the astrophysically interesting range of parameters.

5.2 *The circular orbit case*

The circular case is important both from the pedagogical and physical point of view: (a) it provides us several insights into the problem via a comparatively easier computation; (b) in targetted searches, several known NS in binary systems, including Sco X-1, are essentially in a circular orbit; (c) for blind searches, present and near future processing power is likely to allow us to search over a reasonable parameter space mainly for emitters orbiting a companion with $e = 0$.

For circular orbits, the expression of the phase (20) simplifies considerably. We have $e = 0$ and ψ and α combine additively into a single parameter which we redefine again as α for the sake of simplicity; in effect we put $\psi = 0$. Then X is just the projected radius of the orbit which we denote by A. We therefore have just 3 search parameters for which a discrete mesh of filters is required: $\boldsymbol{\Lambda} = (\kappa\,, A\,, \Omega\,, \alpha)$ and $\boldsymbol{\lambda} = (A\,, \Omega\,, \alpha)$. The phase (20) is rewritten as

$$\tilde{\Phi} = \kappa u + A \cos(\Omega u + \alpha)\,. \tag{21}$$

The scaled metric $\tilde{g}_{\alpha\beta}$ is now a 4×4 matrix, and we compute it from eqs (12) and (21).

The exact analytical expression of $\tilde{V}_{\mathcal{P}} = \sqrt{\det ||\tilde{\gamma}_{jk}||}$ is very complex and not illuminating. However, as discussed in the previous section, it is possible to compute $\det ||\tilde{\gamma}_{jk}||$ in a closed form in the two relevant regimes: (i) $\Omega \gg 1$, the limit of several orbits during the observation time T, and (ii) $\Omega \ll 1$, the limit of monitoring fraction of an orbit. In the limit $\Omega \gg 1$, the proper volume element in scaled coordinates is:

$$\sqrt{\det ||\tilde{\gamma}_{ij}||} = \frac{A^2}{\sqrt{96}} + o(\Omega^{-1}, A^3)\,. \tag{22}$$

From numerical computations it is found that even for $\Omega \gtrsim 10$, which corresponds to about 2 orbits completed during an observation time T, the above expression gives reasonably accurate results. The approximation improves further with large Ω.

The (unscaled) proper volume is given by (we have multiplied by the appropriate power of $2\pi f_{\max} T$)

$$V_{\mathcal{P}} = \frac{\pi}{6\sqrt{6}} \left(\frac{2\pi f_{\max}}{c}\right)^3 [a_{p,\max}^3 - a_{p,\min}^3](\omega_{\max} - \omega_{\min})T\,, \tag{23}$$

where the subscripts 'max' and 'min' specify the maximum and minimum respectively, of the ranges of the parameters. Notice that the factor $2\pi f_{\max}/c$ is the maximum wavenumber of the gravitational wave that we want to detect. The main point in eq. (23) is to observe how the volume scales. The number of filters increases linearly in the observation time T, so hierarchical searches based on T will not work effectively (compare this to the case of the all sky all frequency search for isolated pulsars where the patches scale as T^5). The volume is proportional to the cube of the size of the projected orbit along the line of sight a_p. So knowing this parameter will greatly reduce the computational load.

In the opposite limit of $\Omega \ll 1$, we obtain the following volume element

$$\sqrt{\det ||\gamma_{ik}||} = \frac{|\cos\alpha|}{3628800\sqrt{35}} A^2 \Omega^8 + o(\Omega^9, A^3). \tag{24}$$

Figure 1 shows the square root of the determinant of the metric computed numerically. It is seen that in the two regimes, the relevant approximations are quite accurate. Moreover, there is only a small range of Ω around 1 radian, where the approximations are not so accurate.

By integrating eq. (24) over the parameter range and following steps similar to the previous case, we obtain the volume:

$$\begin{aligned} V_{\mathcal{P}} = & \frac{1}{24494400\sqrt{35}} \left(\frac{2\pi f_{\max}}{c}\right)^3 [a_{p,\max}^3 - a_{p,\min}^3] \\ & \times \left[(\omega_{\max} T)^9 - (\omega_{\min} T)^9\right]\,. \end{aligned} \tag{25}$$

Following the same scheme as in the previous section, we can obtain the total volume of the parameter space, when no prior information about the source parameters is available:

$$\begin{aligned} V_{\mathcal{P}} & \simeq 0.6 \left(\frac{f_{\max}}{1\,\mathrm{kHz}}\right)^3 \left(\frac{a_{p,\max}}{10^{11}\,\mathrm{cm}}\right)^3 \left(\frac{\omega_{\max}}{10^{-4}\,\mathrm{rad/sec}}\right)^9 \left(\frac{T}{1\,\mathrm{hr}}\right)^9 \\ & \simeq 3.4 \times 10^4 \left(\frac{f_{\max}}{1\,\mathrm{kHz}}\right)^3 \left(\frac{a_{p,\max}}{10^{13}\,\mathrm{cm}}\right)^3 \left(\frac{\omega_{\max}}{10^{-7}\,\mathrm{rad/sec}}\right)^9 \left(\frac{T}{1\,\mathrm{month}}\right)^9 . \end{aligned} \tag{26}$$

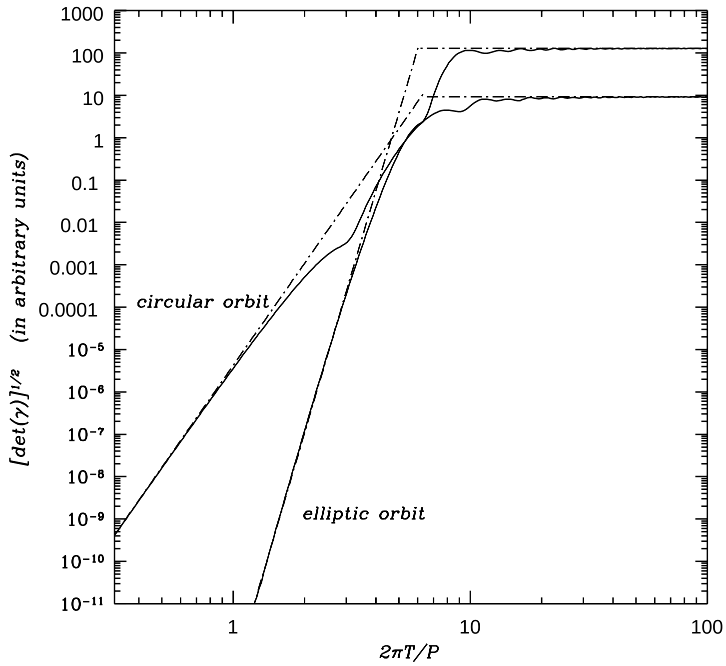

Figure 1. The plot shows the proper volume element $\sqrt{\det||\gamma_{jk}||}$, in arbitrary units, as a function of the dimensionless orbital frequency parameter $\Omega \equiv \omega T$ for circular and elliptical orbits. Note that the normalizations for the two cases are different; they are chosen such that the values of $\sqrt{\det||\gamma_{jk}||}$ are comparable. The numerical results are shown with a solid line, while the asymptotic analytical expressions for $\Omega \gg 1$ and $\Omega \ll 1$ are shown with dotted-dashed lines. Notice that for $\Omega \geq 20$ the asymptotic expansion is indistinguishable from the full expression. In the opposite limit, $\Omega \ll 1$, we observe that $\sqrt{\det||\gamma_{jk}||} \propto \Omega^8$ for the circular orbit and $\propto \Omega^{19}$ for the elliptical orbit.

5.3 *The elliptical orbit ($e > 0$)*

We take the expansion of the eccentric anomaly E up to 7th order in e, which means we consider 7 harmonics in ω. The volume that we obtain is also correct up to this order in e. Since now there are two more parameters, the problem is more complex than in the circular case and it is impossible to obtain a closed form expression of the determinant. We present here an approximate expression of the volume element, and therefore the number of filters, in the asymptotic limit $\Omega \gg 1$.

In the coordinates $A, \psi, e, \Omega, \alpha$ the volume element is

$$\sqrt{\det||\tilde{\gamma}_{jk}||} = \frac{A^4}{32\sqrt{6}}\left[e - \frac{3}{4}e^3 - \frac{41}{256}e^5 + \frac{\cos 2\psi}{32}(4e^3 - e^5) - \frac{\cos 4\psi}{256}e^5\right]. \tag{27}$$

Comparing the former expression with the numerical evaluation of the full determinant it turns out that eq. (27) is accurate within a few per cent even if the number of orbits completed during the time T is just about 2 or 3.

In order to obtain the proper volume of the parameter space, we integrate eq. (27) over the parameter range and multiply by an appropriate power of the scaling factor

$$V_{\mathcal{P}} = \frac{\pi^2}{160\sqrt{6}} \left(\frac{2\pi f_{\rm max}}{c}\right)^5 [a_{p,{\rm max}}^5 - a_{p,{\rm min}}^5] (\omega_{\rm max} - \omega_{\rm min}) T \; F(e_{\rm max}), \tag{28}$$

where

$$F(e) = e^2 \left(1 - \frac{3}{8}e^2 - \frac{41}{768}e^4\right) . \tag{29}$$

We expect that eq. (29) will be correct up to $e \sim 0.8$. We also checked how well the leading order term e^2 approximates $F(e)$, and we found that up to $e = 0.5$ and $e = 0.8$ (as reference values), they agree within $\simeq 10\%$ and $\simeq 35\%$, respectively.

For blind searches, the volume of the parameter space is

$$\begin{aligned} V_{\mathcal{P}}^{(e)} \simeq 2.5 \times 10^{23} & \left(\frac{f_{\rm max}}{1\,{\rm kHz}}\right)^5 \left(\frac{a_{p,{\rm max}}}{10^{11}\,{\rm cm}}\right)^5 \left(\frac{\omega_{\rm max}}{10^{-3}\,{\rm rad/sec}}\right) \left(\frac{T}{10^7\,{\rm sec}}\right) \\ & \times \left(\frac{\alpha_{\rm max}}{2\pi}\right) \left(\frac{\psi_{\rm max}}{2\pi}\right) \left(\frac{e_{\rm max}}{0.5}\right)^2 , \end{aligned} \tag{30}$$

where, for the sake of simplicity, we have retained only the leading order term in e, in eqs (28) and (29), and have considered the same typical values for parameter ranges as in the circular case. The total number of filters now is

$$\mathcal{N} \simeq 1.1 \times 10^{27} \left(\frac{V_{\mathcal{P}}^{(e)}}{10^{23}}\right) \left(\frac{\rho_5(\mu)}{1.12 \times 10^4}\right) . \tag{31}$$

It is clear that in this case we will need some information about the system to reduce the computational costs. Clearly the steep dependence on a_p to the power 5 means that we could cut down the computational costs substantially, if we had a good estimate of this parameter. Also there is steep dependence on the maximum frequency of the GW we want to detect. If we reduce our expectations by a factor half in the $f_{\rm max}$, the computing cost comes down by as much as a factor of ≈ 30. These are the crucial parameters which govern the computational costs. $\mathcal{N}$ still scales linearly with ωT. For sufficiently small values of the eccentricity, it scales quadratically with e.

5.4 *Computational costs for targetted searches*

In this section we investigate the computational costs involved in searching for the X-ray source Sco X-1 and the 44 radio pulsars in binaries listed in [19]. Some of the parameters are known within error bars from X-ray and radio observations. One then integrates the volume element within the given error bars to obtain the volume and the computational cost. If the error bars are very narrow, within inter-filter distance, boundary effects are crucial in computing the costs and must be incorporated into the calculation. The problem of boundary effects is quite involved, which we do not discuss here, but refer to our detailed paper [27]. The costs mentioned here include the boundary effects.

Sco X-1 is at a distance of 2.8 ± 0.3 kpc and the system is essentially in a circular orbit with period $P = 0.787313\,(1)$ days and radial velocity $v_r = 58.2\,(3.0)$ km/sec. The phase of the orbit is known within ± 0.1 radians and the maximal frequency is approximately $f_{\max} \approx 600$ Hz [15]. These observations in our variables give, $a^{\rm proj} = P v_r/2\pi \simeq 6.3 \times 10^5$ km and $\omega \simeq 9.2 \times 10^{-5}$ rad/sec. Integrating within the error bars we obtain the number of filters as

$$N_f \simeq 2.5 \times 10^6 \left(\frac{f_{\max}}{600\,\mathrm{Hz}}\right)^3 \left(\frac{T}{10^5\,\mathrm{sec}}\right) \left[\frac{\rho_3(\mu)}{125}\right] . \tag{32}$$

Sco X-1 could be marginally detectable by the first generation of instruments for coherent integration times of a few years (here we consider the fiducial time $T = 10^7$ sec) [9,15]. We can enquire about the accuracy with which we must know the orbital parameters so as only a single Doppler correction is necessary. It turns out that one needs to know all the parameters within one part in 10^6 for this purpose. For the enhanced configuration of detectors only a few days of coherent integration is necessary [9] and the requirements become one order of magnitude less stringent.

The computational costs for the 44 radio pulsars are as follows: The number of filters required for an observation time of 1 year and with a mismatch at 3% is computed. Out of the 44 pulsars, 7 emit at GW frequencies (taken to be twice the radio frequency) less than 10 Hz and thus lie outside the detector bandwidth. Out of the remaining 37 pulsars, 23 need less than 10 filters, 6 need between 10 and 10^3 filters, 6 need between 10^3 and 10^8 filters and 2 need more than 10^8 filters.

6. Conclusions

In this article, the data analysis problem for CGW sources has been discussed with special emphasis on the problem of a CGW source orbiting a companion. It is found that the computational cost for a 'blind' search can be prohibitive and the data analysis is therefore restricted by the available computing power. Targetted searches however are possible if sufficient information is available about the source. Here we have not considered intrinsic changes in frequency of the source, such as, spin down. These effects need to be included in a future programme. One expects the cost to increase enormously, as in the search for isolated NS [11]. In order to deal with this enormous computational burden alternative data analysis strategies need to be devised. Hierarchical search is one such strategy. Such strategies are being designed for the isolated NS [17,18]. One needs to design similar strategies for the CGW source in a binary. This problem will be addressed in future.

Perhaps a radically new approach to the problem is called for. One alternative could be to develop a transform which quickly processes the data by applying the necessary Doppler (and other corrections) in relatively less number of operations. The problem is analogous to the FFT. The FFT 'works' because there is the cyclic group of roots of unity at the basis of the algorithm. For the isolated NS whose direction is unknown, the rotation group is the relevant one. Developing a transform using the symmetries of the group could well turn out to be a worthwhile approach to consider.

References

[1] A Abramovici *et al*, *Science* **256**, 325 (1992)
[2] C Bradaschia *et al*, *Nucl. Instrum. Methods Phys. Res.* **A289**, 518 (1990)
[3] K Danzmann, in *Gravitational Wave Experiments* edited by E Coccia, G Pizzella and F Ronga (World Scientific, Singapore, 1995) p. 100–111
[4] K Tsubono, in *Gravitational Wave Experiments* edited by E Coccia, G Pizzella and F Ronga (World Scientific, Singapore, 1995) p. 112–114
[5] R J Sandeman *et al*, *A.I.G.O. Prospectus* (1997) unpublished
[6] P L Bender *et al*, *LISA Pre-Phase: A Report*, Second Edition, MPQ 233 (1995)
[7] K S Thorne, in *Proceedings of the Snowmass 95 Summer Study on Particle and Nuclear Astrophysics and Cosmology* edited by E W Kolb and R Peccei (World Scientific, Singapore, 1995) p. 398
[8] E Flanagan, in *Gravitation and relativity: At the turn of the millennium* edited by N Dadhich and J Narlikar (IUCAA, Pune, 1998) p. 177–198
[9] B F Schutz, *Gravitational wave astronomy*, in press, gr-qc/9911034
[10] B F Schutz, in *The Detection of Gravitational Waves* edited by D Blair (Cambridge University Press, Cambridge, England, 1989) p. 406–427
[11] P R Brady, T Creighton, C Cutler and B F Schutz, *Phys. Rev.* **D57**, 2101 (1998)
[12] B Owen, L Lindblom, C Cutler, B F Schutz, A Vecchio and N Anderson, *Gravitational waves from hot young rotating neutron stars*, gr-qc/9804044
[13] J Papaloizou and J E Pringle, *Mon. Not. R. Astron. Soc.* **184**, 501 (1978)
[14] R V Wagoner, *Ap. J.* **278**, 345 (1984)
[15] L Bildsten, *Ap. J.* **501**, L89 (1998)
[16] G Ushomirsky, C Cutler and L Bildsten, *Deformations of accreting neutron star crusts and gravitational wave emissions*, submitted, astro-ph/0001136
[17] P R Brady and T Creighton, *Searching for periodic sources with LIGO II: Hierarchical searches*, submitted, gr-qc/9812014
[18] B F Schutz and M A Papa, in *Gravitational waves and experimental gravity* (Proceedings of Modiond, 1999) (Editions Frontieres, Orsay, 1999) gr-qc/9905018
[19] J H Taylor, R N Manchester and A G Lyne, *Ap. J.* **88**, 529 (1993)
J H Taylor, R N Manchester, A G Lyne and F Camillo, unpublished work. The version of the catalogue used in this paper is actually the electonic, up-dated version of the orginal one. It is *Catalog of 706 pulsars*, avaliable via anonymous ftp at pulsar.princeton.edu. Notice that after the publication of the catalogue of 706 pulsars more orbital system has been found
[20] S V Dhurandhar, D G Blair and M E Costa, *Astron. Astrophys.* **311**, 1043 (1996)
[21] S D Mohanty, I S Heng, D G Blair, S V Dhurandhar, M Tobar and E Ivanov, *Mon. Not. R. Astron. Soc.* **301**, 469 (1998)
[22] D R Lorimer, *Binary and Millisecond Pulsars*, Living Reviews in Relativity (1998) vol. 1, p. 10
[23] S V Dhurandhar and B S Sathyaprakash, *Phys. Rev.* **D49**, 1707 (1994)
[24] R Balasubramanian, B S Sathyaprakash and S V Dhurandhar, *Phys. Rev.* **D53**, 3033 (1996)
[25] B J Owen, *Phys. Rev.* **D53**, 6749 (1996)
[26] I Jones and B F Schutz, private communication
[27] S V Dhurandhar and A Vecchio, in preparation